ID-1342

Modeling of Brittle Particle Fracture in Particle Reinforced Ductile Matrix Composites by 3D-Unit Cells

Anton Eckschlager, Wensheng Han, Helmut J. Böhm
Christian Doppler Laboratory for Functionally Oriented Materials Design at the Institute of Lightweight Structures and Aerospace Engineering, Vienna University of Technology, A-1040 Vienna, Austria

SUMMARY: A successive cracking model of brittle reinforcements is presented for particle reinforced ductile matrix composites. The three-dimensional unit cell approach describing specific arrangements of spherical inclusions uses the finite element method for evaluating the microscale stresses and strains. Appropriate predefined fracture surfaces are employed to allow brittle cleavage controlled by Weibull-type fracture probabilities evaluated from the current stress distributions within the particles.
For a first investigation uniaxial loading of a SiC reinforced Al2618-T4 matrix is simulated. Only particle fracture is modeled, other damage processes, i.e. interfacial decohesion and matrix failure, being neglected. Results showing the cleavage of a number of particles, the evolution of the fracture probabilities of the particles and the macroscopical response are presented.

KEYWORDS: Metal Matrix Composites, Particle Reinforced Composites, Particle Fracture, Unit Cell Models, Weibull Fracture Probability.

INTRODUCTION

Initiation and progress of damage in metal matrix composites (MMCs) subjected to mechanical loading can take place via three basic local processes, viz. matrix failure, reinforcement failure and interfacial decohesion. Depending on the strength as well as stiffness properties of the MMCs' constituents and their geometrical arrangement these failure mechanisms can act independently or in interaction.

Numerous unit cell studies resolving the local stress and strain fields in particle reinforced MMCs have been reported for planar or axisymmetric model geometries, see e.g. [1,2,3]. Micromechanically based modeling work on microscale damage in particle reinforced MMCs, using both numerical and analytical approaches, has also been carried out, compare e.g. [4,5,6]. Recent results [7,8], however, have pointed out the limitations of two-dimensional models for particle reinforced composites with the out-of-plane constraints introduced by plane stress and plane strain states. Axisymmetric cell models and cubic arrangements of particles are more realistic, but they are obviously limited to highly regular microgeometries. Accordingly, it is of significant interest to study microscale damage in particulate reinforced MMCs by three-dimensional models using irregular particle arrangements.

In a number of MMC systems brittle reinforcement failure tends to be the primary microscale damage mechanism [6]. Experiments mostly show that cracks run through the particles' centers, depending on particle size and shape [9], and their orientation is preferentially normal to the applied loading direction [10,11]. In the following a three-dimensional multi-inclusion unit cell modeling method for studying this damage mechanism is presented.

MULTI-INCLUSION UNIT CELL AND PARTICLE CRACKING MODELS

To obtain models that can be handled by the available computational resources, appropriate simplifications had to be introduced. For the particles isotropically elastic material behavior is assumed and for the matrix a J_2-continuum plasticity model is used with a modified Ludwik hardening law of the type

$$\sigma_{\mathrm{y}} = \sigma_{\mathrm{y,0}} + h\varepsilon_{\mathrm{eq,p}}{}^{n} . \tag{1}$$

Here σ_{y} is the actual flow stress, $\sigma_{\mathrm{y,0}}$ the initial yield stress, and $\varepsilon_{\mathrm{eq,p}}$ the accumulated equivalent plastic strain, while h and n stand for the hardening coefficient and the hardening exponent, respectively. The material parameters used in the analysis are listed in Table 1, where E denotes the Young's modulus and ν the Poisson's ratio. Initially stress free and virgin material is assumed for all analyses.

Table 1: Material parameters used for the elastoplastic SiC/Al2618-T4 MMC (modified Ludwik hardening law for the matrix), which follow closely the data given in [6].

Material	E [GPa]	ν [1]	σ_{y} [MPa]	h [MPa]	n [1]	m [1]	σ_{f} [GPa]
Al2618-T4 matrix	70.0	0.30	184.0	722.7	0.49	-	-
SiC reinforcement	450.0	0.17	-	-	-	3.0	1.0

In addition, perfect bonding between the particles and the matrix is assumed, neglecting any interfacial effects during the load history. Approximating the microgeometry of a real composite by a finite number of brittle particles periodically embedded in an elastoplastic matrix also implies an idealization in that the failure of a single inclusion in the unit cell actually corresponds to a three-dimensional periodically repeating pattern of failed particles. In the model shown in Figure 1 — 15 spherical reinforcements of equal size in a unit cell for a total particle volume fraction of ξ=6.3% — the failure of one inclusion describes the simultaneous fracture of approximately 6.7% of all particles in the composite.

The modeling of particle failure is realized by a node release technique. Crack planes are predefined in perpendicular orientation to the direction of the applied macroscopic stress, assuming that a critical initial flaw should have this orientation for brittle failure, and positioned to pass through the particle's center. Cracks are assumed to open instantaneously once a chosen maximum fracture probability is exceeded. Therefore, local stress field perturbations caused by stress redistribution due to the failure of neighboring particles, which may influence the crack orientation, are neglected. Reinforcement failure always leads to the total splitting of the particle, and further crack growth into the matrix and/or along an interface is not allowed.

For obtaining the probability of failure ${}^{j}P_{\mathrm{fr}}^{(p)}$ of particle j the following Weibull description is chosen [12]:

$${}^{j}P_{\mathrm{fr}}^{(p)} = 1 - \exp\left\{ -\frac{1}{V_0^{(p)}} \int_{{}^{j}V^{(p)}:\sigma_1>0} \left(\frac{\sigma_1(x)}{\sigma_{\mathrm{f}}^{(p)}} \right)^{m} dV \right\} \tag{2}$$

Here m is the Weibull modulus of the particles, $s_1(x)$ stands for the distribution of the maximum principal stress within inclusion j, $s_f^{(p)}$ is the characteristic strength of the particles and ${}^jV^{(p)}:s_1(x)>0$ stands for that part of the particle's volume in which s_1 is tensile. The reference volume $V_0^{(p)}$ was set equal to the particles' volume. Values for the material parameters used here, which correspond to SiC particulates, are listed in Table 1. For simplicity, in the present study failure of the j-th particle was assumed to take place when the associated fracture probability ${}^jP_{\mathrm{fr}}^{(p)}$ exceeded a value of 0.632.

IMPLEMENTATION

The phase arrangement shown in fig. 1a is a unit cell model with 15 equally sized and identically shaped particles that is employed to represent a volume element of an Al2618-T4 MMC with spherical SiC reinforcements. The evaluation of the microscale stress and strain fields in the unit cells was carried out with the finite element code ABAQUS [13], modified tetrahedral elements with quadratic shape functions (3D10M) being used. The total number of elements in the model reached about 40000.

For easier meshing during the development phase of the algorithm "randomly pruned cube arrangements" were employed: the cube shaped unit cell was partitioned into 64 (i. e. 4×4×4) identical subvolumes, 15 of which were randomly selected to contain centered spherical particles of equal size that are embedded in matrix material. The other 49 subvolumes where wholly assigned to the elastoplastic matrix phase. This method evidently gives rise to phase arrangements that are much more irregular than the sc, fcc or fcc arrays frequently used in the literature (see e.g. [14]), but the interparticle distances remain relatively large and the particle positions show patterns of layering.

Periodic boundary conditions were implemented and displacement controlled geometrically nonlinear analyses describing loading by uniaxial tension were carried out. The node release mechanism for particle failure under control of the Weibull fracture probabilities as described above was realized via the ABAQUS user subroutines `MPC`, `UVARM` and `UEXTERNALDB`. The evaluation of the particles' Weibull fracture probabilities as defined in eqn.(2) made use of a feature of ABAQUS that allows the approximate calculation of volume integrals of some function f over some subvolume, in this case particle j, by a weighted sum of the type

$$\langle f \rangle^{(j)} = \frac{1}{V^{(j)}} \int_{V^{(j)}} f(x)dV \approx \frac{1}{V^{(j)}} \sum_{l=1}^{N^{(j)}} f_l V_l \qquad \text{with} \qquad \sum_{l=1}^{N^{(j)}} V_l = V^{(j)} \tag{3}$$

Here f_l stands for the value of the function $f(x)$ at the integration point l, which is weighted by the volume V_l associated with this integration point. $N^{(j)}$ is the total number of integration points within particle j.

DISCUSSION

Simulations of uniaxial tensile loading up to overall nominal strains of approximately 22% were carried out for the phase arrangement depicted in fig. 1. Applying the load in 1-direction and using a preselected critical Weibull fracture probability of 0.632, brittle cleavage of seven particles was predicted by the model. The sequence of failure was `INCLB15`, `INCLA09`, `INCLB14`, `INCLD03`, `INCLC07`, `INCLC01` and INCLD05, the final deformed state being shown in fig. 1b.

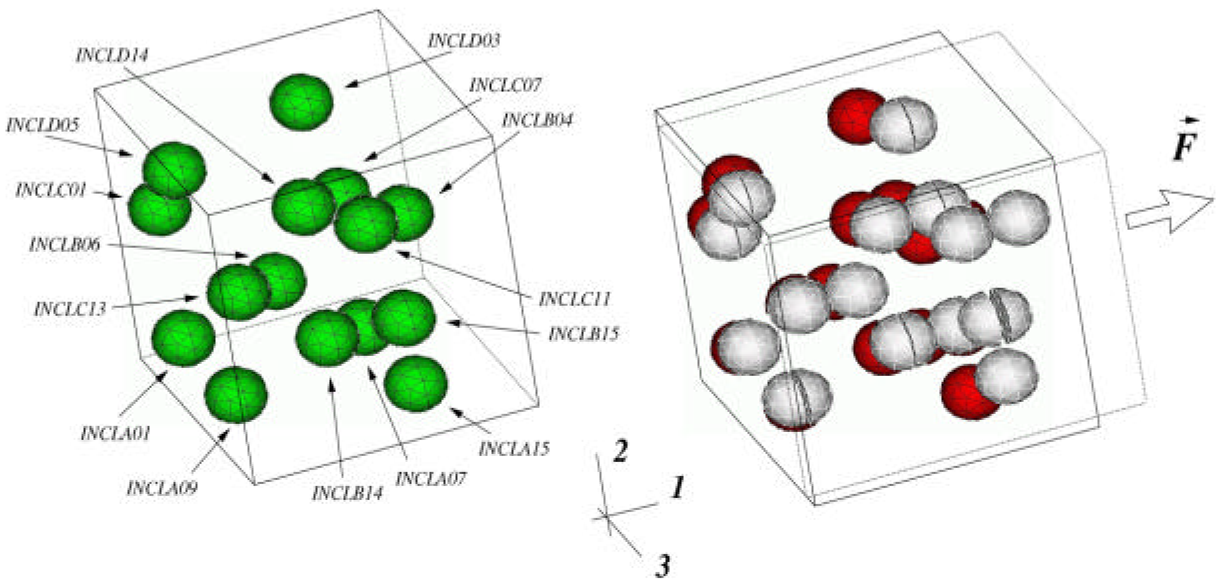

a) **b)**

Figure 1: a) Unit Cell with 15 spherical particles of identical size in a randomly pruned cubic arrangement (volume fraction ξ=6.3%), b) loaded uniaxially in the 1-direction (red shade and solid lines mark initial state, grey shade and dotted lines mark deformed state). Material modeled is SiC/Al2618-T4 MMC.

The evolution of the Weibull fracture probabilities for the above case is shown in Figure 2. Four of the five particles represented there, `INCLC01`, `INCLB15`, `INCLB14` and `INCLA09`, fail within the studied load sequence, whereas one inclusion, `INCLD14`, is obviously not subjected to sufficiently high stresses. A nonlinear dependence of the particles' Weibull fracture probability on the overall strain is apparent once the matrix starts yielding and this is markedly influenced by the particles' positions. The first failure of an inclusion, `INCLB15`, unloads the direct neighbor `INCLB14`, whereas other inclusions carry more load after stress redistribution. Continuing in the reinforcement failure sequence `INCLA09`, a close neighbor to `INCLB15` (considering the periodicity conditions) fractures and its failure decreases the fracture probability of particle `INCLC01` but increases that of `INCLB14`, both of which are positioned relatively far away from the fractured inclusions. With further loading, the limit load for `INCLB14` is reached.

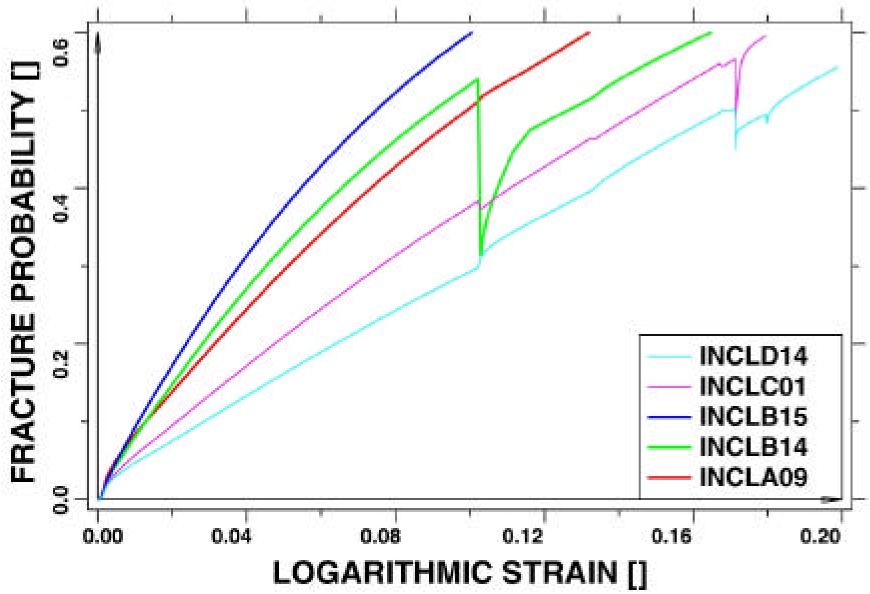

Figure 2: Predicted evolution of Weibull fracture probabilities under uniaxial tensile loading for selected particles in the arrangement introduced in fig. 1. For the failed particles the highest fracture probabilities obtained in the increment before cleavage occurred (the critical Weibull fracture probability used was 0.632) are shown.

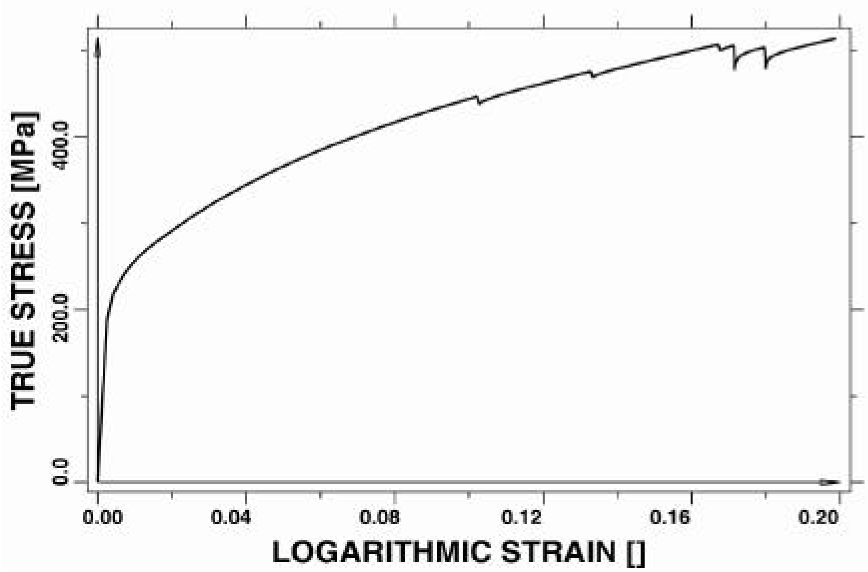

Figure 3: Overall uniaxial stress-strain relation predicted by the unit cell arrangement shown in fig. 1 of a SiC/Al2618-T4 MMC (ξ=6.3%). A Weibull fracture probability of 0.632 was used to trigger particle cracking.

A unit cell's overall response is shown in the stress vs. strain diagram Figure 3. Sudden overall stiffness reductions occur at five different strain values. Beginning with lower strains the first three of them correspond to cleavage of single inclusions, whereas the other two are caused by the failure of two particles in quick succession. As mentioned before, the high intensity of the drops in overall stiffness is due to the unit cell modeling concept, within which the fracture of one particle in the model corresponds to the cleavage of 6.7% of all inclusions in the modeled composite.

CONCLUSION

A successive cracking model of brittle reinforcements for a particulate reinforced MMC has been implemented successfully. The three-dimensional unit cell approach, which employs the finite element method for evaluating the microscale stresses and strains, allows to follow the sequence of failure of a number of particles during the simulations without user intervention. Brittle cleavage, controlled deterministically by a Weibull-type particle fracture probability, was modeled as taking place instantaneously along appropriate predefined fracture surfaces and was realized by a node release technique.

For simplicity "randomly pruned cube" microgeometries were used in the initial studies discussed above. At present, work is in progress that is based on more realistic particle arrangements generated by variants of the random sequential adsorption algorithm [8,15]. Another development currently in hand involves Monte Carlo procedures for triggering the failure of particles on the basis of their Weibull fracture probabilities, which considerably increases the realism of the simulations.

In the short term the number of particles in models of the above types, however, will remain limited to 15 to 20 on account of the high computational requirements of the procedures. Because the microscale stresses and strains in the particles may be noticeably influenced by load redistribution effects due to the failure of neighbouring reinforcements it is desirable to improve the method by selecting fracture surfaces during incrementing, which will require remeshing just before a particle fails.

ACKNOWLEDGEMENTS

The authors wish to acknowledge the financial support of the Christian Doppler Research Society and helpful discussions with Prof. F. G. Rammerstorfer.

REFERENCES

1. H. Berns, A. Melander, D. Weichert, N. Asnafi, C. Broeckmann, A. Gross-Weege, New material for cold forging tools, *Comput. Mater. Sci.* **11**(1998) 166-188.
2. S. Gosh, S. Moorthy, Particle fracture simulation in non-uniform microstructures of metal-matrix composites, *Acta mater.* **46**(1998) 965-982.

3. S. R. Nutt, A. Needleman, Void nucleation at fiber ends in Al-SiC composites, *Scripta metall.* **21**(1987) 705-710.
4. K. Tohgo, G. J. Weng, A progressive damage mechanics in particle-reinforced metal-matrix composites under high triaxial tension, *J. Engng. Mater. Technol.* **16**(1994) 414-420.
5. R. Estevez, E. Maire, P. Franciosi, D. S. Wilkinson, Effect of particle clustering on the strengthening versus damage rivalry in particulate reinforced elastic plastic materials: A 3D analysis from a self-consistent modeling, *Eur. J. Mech. A/Solids* **18**(1999) 785-804.
6. J. LLorca, J. González, Microstructural factors controlling the strength and ductility of particle reinforced metal-matrix composites, *J. Mech. Phys. Sol.* **46**(1998) 1-28.
7. T. Iung, M. Grange, Mechanical behavior of two-phase materials investigated by the finite element method: necessity of three-dimensional modeling, *Mater. Sci. Engng.* **A201**(1995) L8-L11.
8. H. J. Böhm, W. Han, Comparison between three-dimensional and two-dimensional statistics-based unit cell models for particle reinforced MMCs, *to be published in Modell. Simul. Mater. Sci. Engng.*
9. K. Wallin, T. Saario, K. Törrönen, Fracture of brittle particles in a ductile matrix, *Int. J. Fract.* **32**(1987) 201-209.
10. N. M. Mawsouf, A micromechanical mechanism of fracture initiation in discontinuously reinforced metal matrix composites, *Mater. Charact.* **44**(2000) 321-327.
11. R. Pandorf, Beitrag zur FE-Simulation des Kriechens partikelverstärkter Metallmatrix-Verbundwerkstoffe, *VDI Fortschritt-Berichte, Reihe 5*, **585**(2000).
12. W. Weibull, A Statistical Distribution Function of Wide Applicability, *J.Appl. Mech.* **18**(1951) 293-298.
13. ABAQUS/Standard V.5.8, Hibbitt, Karlsson and Sorensen Inc., Pawtucket, RI, 1998.
14. E.Weissenbek, H. J. Böhm, F. G. Rammerstorfer, Micromechanical investigations of arrangement effects in particle reinforced metal matrix composites, *Comput. Mater. Sci.*, **3**(1994) 263-278.
15. M. Rintoul, S. Torquato, Reconstruction of the Structure of Dispersions, *J. Colloid Interf. Sci.*, **186**(1997) 467-476.